Magnetic properties of Ni-Mo single-crystal alloys; theory and experiment

1998 J. Phys.: Condens. Matter 10 11773

(http://iopscience.iop.org/0953-8984/10/50/016)

J. Phys.: Condens. Matter **10** (1998) 11773–11780. Printed in the UK PII: S0953-8984(98)93629-3

Magnetic properties of Ni–Mo single-crystal alloys; theory and experiment

Subhradip Ghosh†§, Nityananda Das† and Abhijit Mookerjee‡‖

† S N Bose National Centre for Basic Sciences, JD Block, Sector 3, Salt Lake City, Calcutta 700091, India

‡ Department of Physics, Indian Institute of Technology, Kanpur 208016, India

Received 23 April 1998, in final form 24 September 1998

Abstract. The magnetizations of $Ni_{1-x}Mo_x$ single crystals with $x = 4$, 6, 8 and 10% by weight have been measured at 4.2 K using a vibrating-sample magnetometer and a superconducting quantum interference device (SQUID). The magnetizations of the alloy at these low concentrations and at 0 K have been theoretically determined by using the tight-binding linearized muffin-tin orbital method coupled with augmented-space recursion. The theoretical data are compared with the experiment.

1. Introduction

The equilibrium phase diagram of the $Ni_{1-x}Mo_x$ system exhibits a continuous face-centred-cubic disordered solid solution over the range $0 < x \leqslant 0.12$. The alloy shows a series of ordered phases at higher concentrations. The phase diagram for the NiMo alloy system has been given by Das *et al* [1]. They have studied the phase diagram for higher concentration ranges using the tight-binding linearized muffin-tin approximation (TB-LMTO) method based on the local density approximation (LDA), proposed by Andersen and Jepsen [2]. As far as we are aware, no similar study of the disordered regime has been carried out in detail. In this communication, we shall report such a study, using the same TB-LMTO methodology as before but combining this with the augmented-space recursion proposed by one of us [3] to take care of the disorder configuration averaging. We shall evaluate the local magnetization as a function of the Mo concentration. Simultaneously, we shall measure the magnetization of four alloy systems in this disordered alloy regime ($x = 0.04$, 0.06, 0.08 and 0.1). In parallel, we shall compare our results with experimental work on the magnetization and Curie temperatures of single crystals of NiMo [4].

2. Theoretical details

The TB-LMTO method has been described in great detail earlier [5]. We refer the reader to monograph [5] for technical details.

Description of magnetic phases within the local spin-density approximation (LSDA) involves the study of the evolution of local magnetic moments in the vicinity of ion cores

§ Author to whom any correspondence should be addressed. E-mail: subhra@boson.bose.res.in.

‖ On sabbatical leave from: S N Bose National Centre for Basic Sciences, JD Block, Sector 3, Salt Lake City, Calcutta 700091, India.

0953-8984/98/5011773+08$19.50

because of the distribution of the valence electron charge. Each lattice site in the face-centred-cubic structure is occupied by an ion core—in our case, randomly by either Ni or Mo. We shall associate a cell or a sphere with each ion core and assume that the charge contained in the sphere belongs to that ion core alone. Ideally, such cells or spheres should not overlap. In the traditional Kohn–Korringa–Rostoker (KKR) method this is certainly the case. However, in the atomic sphere approximation (ASA) which we shall use in our TB-LMTO version, this division of space is to a certain extent arbitrary. Within these cells the valence electrons carrying spin σ 'see' a binary random spin-dependent potential $V_\sigma^\lambda(\boldsymbol{r})$, where $\lambda =$ Ni or Mo and $\sigma = \uparrow$ or $\downarrow$.

The charge density within the cells can be obtained from the partially averaged Green functions:

$$\rho_\sigma(r) = -(1/\pi)\,\mathrm{Im}\sum_L \int_{-\infty}^{E_F} \left[x\langle\langle G_{LL}^{\mathrm{Mo},\sigma}(r,r,E)\rangle\rangle + (1-x)\langle\langle G_{LL}^{\mathrm{Ni},\sigma}(r,r,E)\rangle\rangle\right] \mathrm{d}E$$

where $\langle\langle G_{LL}^{\mathrm{Mo},\sigma}(r,r,E)\rangle\rangle$ and $\langle\langle G_{LL}^{\mathrm{Ni},\sigma}(r,r,E)\rangle\rangle$ are partially averaged Green functions, with the site r occupied by a Mo- or Ni-ion core potential corresponding to spin σ. The Mo sites are almost spin independent (except for a very small induced moment) and do not appreciably contribute to local moment densities.

The averaging is done over configurations of the random alloy. A powerful technique for carrying out this averaging is the augmented-space recursion [6]. The method allows us to go well beyond the traditional single-site coherent potential approximations and has been applied successfully to a wide variety of systems [7, 8]. The convergence of the ASR has been established recently [10], so any approximation that we impose on the recursion is controlled by tolerance limits preset by us. The calculations are self-consistent in the LSDA sense.

The initial TB-LMTO potential parameters are obtained from suitable guessed potentials as described in the article by Andersen and Jepsen [2]. In subsequent iterations the potential parameters are obtained from the solution of the Kohn–Sham equation

$$\left\{-\frac{\hbar^2}{2m}\nabla^2 + V^{\nu\sigma} - E\right\}\phi_\sigma^\nu(r_R, E) = 0 \tag{1}$$

where

$$V^{\nu\sigma}(r_R) = V_{\mathrm{core}}^{\nu\sigma}(r_R) + V_{\mathrm{Har}}^{\nu\sigma}(r_R) + V_{\mathrm{xc}}^{\nu\sigma}(r_R) + V_{\mathrm{Mad}}. \tag{2}$$

Here ν refers to the species of atom sited at R and σ is the spin component. The electronic position within the atomic sphere centred at R is given by $r_R = r - R$. The core potentials are obtained from atomic calculations and are available for most atoms.

The Hartree potential needs discussion. Let us denote the atomic sphere centred at R by S_R. If we wish to obtain the Hartree potential within the atomic sphere S_R when an atom of the type ν is sited at R, the configuration space at the site R is projected onto the fixed configuration ν, while the configurations at the remaining sites are, say, random binary. Let us denote the 'average state' by $\{\nu \in R \otimes \emptyset\}$. The reader is referred to Dasgupta *et al* [6] for the details of the configuration notation and the basic augmented-space theorem. We have

$$V_{\mathrm{Har}}^{\nu\uparrow}(r_R) = e^2\int_{S_R}\mathrm{d}^3r'_R\,\frac{\rho_\uparrow^\nu(r'_R)}{|r_R - r'_R|} + \cdots + e^2\sum_{R''\neq R}\int_{S_{R''}}\mathrm{d}^3r'_{R''}\,\frac{\langle\rho(r'_{R''})\rangle}{|r_R - r'_{R''}|}\cdots$$
$$+ e^2\sum_{R''\neq R}\int_{S_{R''}}\mathrm{d}^3r'_{R''}\,\frac{\delta\rho(r'_{R''})}{|r_R - r'_{R''}|}$$

where

$$\delta\rho(r'_{R''}) = \frac{-1}{\pi}\,\mathrm{Im}\int_{-\infty}^{E_F} \mathrm{d}E\,\left[\langle\{r'_{R''}\otimes \mathrm{A}\in R''\otimes\emptyset\}|\tilde{G}(E)\otimes\tilde{M}_{R''}|\{r'_{R''}\otimes \mathrm{A}\in R''\otimes\emptyset\}\rangle\cdots\right.$$
$$\left.-\,\langle\{r'_{R''}\otimes \mathrm{B}\in R''\otimes\emptyset\}|\tilde{G}(E)\otimes\tilde{M}_{R''}|\{r'_{R''}\otimes \mathrm{B}\in R''\otimes\emptyset\}\rangle\right].$$

$\tilde{G}(E)$ is the augmented-space resolvent $(z\tilde{I}-\tilde{H})^{-1}$ and $\tilde{M}_{R''}$ is the configuration operator, e.g. for binary randomness $\tilde{M}_{R''} = I\otimes\cdots\otimes M_{R''}\otimes I\otimes\cdots$ and, if x is the concentration of the A component, it has a representation

$$\begin{pmatrix} 0 & \sqrt{x(1-x)} \\ \sqrt{x(1-x)} & 1-x \end{pmatrix}.$$

The first two terms are identical to the usual expressions for the CPA [11]. Of course, the partially averaged and averaged charge densities in the ASR have the effects of configuration fluctuation of the immediate environment of the atomic site associated with the atomic sphere included. The last term represents configuration fluctuations in the charge densities associated with atomic spheres other than S_R. This correction is taken only up to the nearest-neighbour environment of S_R.

The exchange–correlation potential is a functional of the charge densities $\rho^{\nu\uparrow}(r_R)$ and $\rho^{\nu\downarrow}(r_R)$. We have used the von Barth–Hedin form of the exchange functional.

The treatment of the Madelung potential in a random alloy has always presented problems. We adopt a procedure suggested by Drchal *et al* [12] and regularly used in CPA calculations within the TB-LMTO method. We choose the atomic sphere radii of the components in such a way that they preserve the total volume on average and the individual atomic spheres are almost neutral. This ensures that total charge is conserved, but each atomic sphere carries no excess charge. However, we are careful that such a choice does not violate the overlap criterion of Andersen and Jepsen [2]. In the ASR-LSDA self-consistency loop, there is charge transfer between these spheres; however, at the end of the self-consistency iterations, the spheres are approximately neutral and hence do not contribute to a Madelung energy. This prescription is to an extent *ad hoc*, and there is no guarantee in general that we will be able to find such atomic sphere radii. However, the procedure has proved rather successful in many earlier CPA [12] and ASR [13] calculations on magnetic alloys and we shall adopt it here. For NiMo, the Vegard's law averaged atomic sphere radii are obtained from $r_{\mathrm{Ni}} = 2.602$ au and $r_{\mathrm{Mo}} = 2.922$ au. The atomic radii chosen for negligible charge transfer are shown in table 1.

Table 1. The atomic sphere radii for Ni and Mo with varying concentration of Mo.

x	r_{av}	r_{Mo}	r_{Ni}
0.0200	2.6092	2.9280	2.6018
0.0400	2.6164	2.9300	2.6016
0.0600	2.6235	2.9250	2.6018
0.0800	2.6306	2.9250	2.6017
0.1000	2.6376	2.9220	2.6020
0.1200	2.6446	2.9220	2.6020

The radii are fairly independent of the Mo concentration, with that for Mo being consistently larger than that for Ni.

Recently, an alternative method has been suggested by Korzhavyi *et al* [14] which goes beyond the mean-field approach and includes charge-fluctuation effects very similar to the

ASR treatment of the Hartree potential. We believe that the method suggested is superior to the one that we have adopted, but leave its implementation within the ASR for later work.

As in the CPA calculations, we iterate until the total energy and moments of the charge density converge. In this sense our calculations are self-consistent in the LSDA sense.

For the random ferromagnetic phase, we proceed as follows: we consider all cells to be identical in that they all carry identical average charge densities. We shall borrow the notation of Andersen and Jepsen [2] to write down functions like $\tilde{f}(r_R)$, which are equal to $f(r)$ when r lies in the atomic sphere labelled by R and zero outside. The ferromagnetic charge densities are defined as follows:

$$\rho_1(r) = \sum_R \tilde{\rho}_\uparrow(r_R)$$
$$\rho_2(r) = \sum_R \tilde{\rho}_\downarrow(r_R).$$

The magnetic moment per cell (atom) is then defined by

$$m = (1/N)\int \mathrm{d}^3\boldsymbol{r}\ [\rho_1(r) - \rho_2(r)] = (1/N)\sum_R \int_{r\leqslant S} \mathrm{d}^3 r\ [\tilde{\rho}_\uparrow(r_R) - \tilde{\rho}_\downarrow(r_R)]$$
$$= (1/N)\sum_R \int_{r\leqslant S} \mathrm{d}^3 r\ m_R(r_R).$$

Since all cells are identical, the above calculation need be done only for one typical cell. Within the TB-LMTO-ASA the cells are replaced by inflated atomic spheres and the remaining interstitial space is neglected. The problem is then one of a binary alloy with an almost non-magnetic charge density due to the Mo ion cores and a magnetic one due to the Ni ones.

For the calculation of the component-projected averaged density of states of the ferromagnetic phase we have used a real-space cluster of 400 atoms and an augmented-space shell up to the sixth-nearest neighbour from the starting state. Eight pairs of recursion coefficients were determined exactly and the continued fraction terminated by the analytic terminator due to Luchini and Nex [9]. In a recent paper, Ghosh *et al* [10] have shown the convergence of related integrated quantities, like the Fermi energy, the band energy, the magnetic moments and the charge densities, within the augmented-space recursion. The convergence tests suggested by the authors were carried out to the prescribed accuracies. We noted that at least eight pairs of recursion coefficients were necessary to provide Fermi energies and magnetic moments to the required accuracies. We have reduced the computational burden of the recursion in the full augmented space by using the local symmetries of the augmented space to reduce the effective rank of the invariant subspace in which the recursion is confined [6] and using the seed recursion methodology [15] with fifteen energy seed points distributed uniformly across the spectrum. Both of the reduction techniques have been described in detail in the papers referred to above, and readers are referred to them for details. It is important to emphasize this point, since erroneous statements have been made to the effect that although the augmented-space recursion method is attractive mathematically, it was not feasible to apply it as a computational technique for real alloys. Furthermore, it has been shown [6] that augmented-space recursion with an analytic terminator *always* produces herglotz results†, whether we use the homogeneous

† A function $f(z)$ is called herglotz if (i) its singularities lie on the real axis in the complex z-plane, (ii) its imaginary part is negative in the upper half z-plane and positive in the lower half z-plane and (iii) $f(z) \sim 1/z$ as $z \to \infty$ along the real axis.

disorder model as in this paper or the version including short-ranged order [7] or local lattice distortions [8].

We have chosen the Wigner–Seitz radii of the two constituent atoms Mo and Ni in such a way that the average volume occupied by the atoms is conserved. Within this constraint we have varied the radii such that the final configuration has neutral spheres. This eliminates the necessity of including the averaged Madelung energy part in the total energy of the alloy. The definition and computation of the Madelung energy in a random alloy had excited controversy in recent literature, and to date no satisfactory resolution of the problem exists. Simultaneously, we made sure that the sphere overlap remains within the 15% limit prescribed by Andersen.

The calculations have been made self-consistent in the LSDA sense—that is, at each stage the averaged charge densities are calculated from the augmented-space recursion and the new potential is generated by the usual LSDA techniques. This self-consistency cycle converged in both total energy and charge to errors of the order of 10^{-5}. We have also minimized the total energy with respect to the lattice constant. The quoted results are those for the minimum configuration. No short-ranged order due to chemical clustering has been taken into account in these calculations, nor any lattice distortions due to the size differences between the two constituents.

The estimates of the Curie temperature were obtained from the magnetic pair energies [16]. The pair energies are defined as follows: at two sites labelled r and r' in a completely random paramagnetic background, we replace the potential by that of either the up-spin ferromagnetic Ni or the down-spin ferromagnetic Ni. We shall denote the Green function of this system by $G_{LL}^{\mathrm{Ni},\sigma\sigma'}(r, r, E)$, σ being the spin type at the site r (either $\uparrow$ or $\downarrow$) and σ' that at the site r'. The pair energy is defined as

$$E(R) = \int_{-\infty}^{E_F} \mathrm{d}E\ E[-(1/\pi)\,\mathrm{Im}\,m(G_{LL}^{\mathrm{Ni},\uparrow\uparrow}(r, r, E) + G_{LL}^{\mathrm{Ni},\downarrow\downarrow}(r, r, E)\cdots - G_{LL}^{\mathrm{Ni},\uparrow\downarrow}(r, r, E) - G_{LL}^{\mathrm{Ni},\downarrow\uparrow}(r, r, E))].$$

Here $R = r - r'$. We may either estimate the above directly, or, to increase the accuracy, we may use the orbital peeling method of Burke [17]. The latter is an extension of the recursion method, where small differences of large energies (as in the definition of the pair energy) are obtained directly and accurately from the recursion continued-fraction coefficients. Note that we have assumed that the dominant contribution to the pair energy comes from the band contribution and the rest approximately cancel out. The simplest Bragg–Williams estimate of the Curie temperature is

$$T_C = (1 - x)E(0)/\kappa_{\mathrm{B}}$$

where

$$E(0) = E(q = 0) \qquad \text{and} \qquad E(q) = \sum_R \exp(\mathrm{i}qR)E(R).$$

Since the pair energy is short ranged, a reasonable estimate of $E(0)$ is

$$\sum_{n<3} Z_n E(R_n)$$

where R_n is the nth-nearest-neighbour vector and Z_n is the number of nth-nearest neighbours. The Bragg–Williams approach overestimates the Curie temperature, and its generalization, the cluster variation method, yields better quantitative estimates. We have restricted ourselves to the Bragg–Williams nearest-neighbour pair energy approximation.

3. Results and discussion

We notice first that in the detailed phase diagram for NiMo [1], the solid-solution phase occupies a small part of the phase diagram below $x = 0.12$ and extends down to the lowest temperatures. In this region there is no transition to an ordered phase at low temperatures. This is the concentration region that we have focused on in this communication.

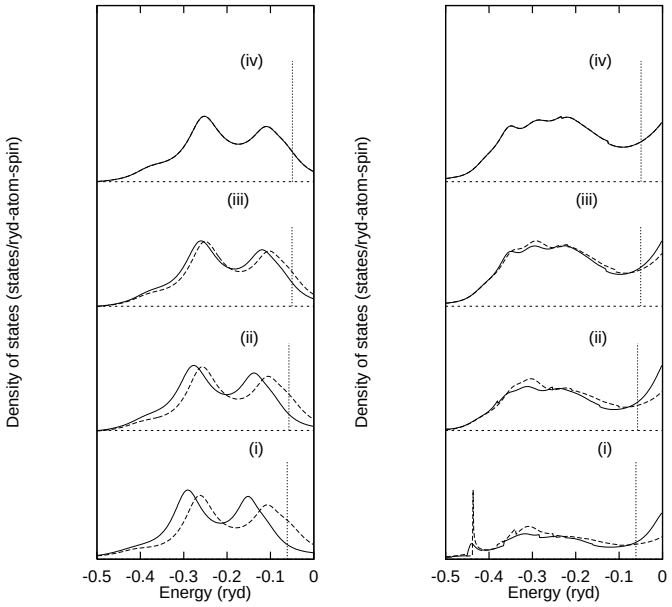

Figure 1. The partial densities of states of Ni (left) and Mo (right) at (i) 2, (ii) 6, (iii) 10 and (iv) 14 at.% of Mo. Dashed curves show the results for the minority spin-states and full curves those for the majority-spin states.

Figure 1 shows the partial densities of states for Ni and Mo. The full curves show the majority-spin partial densities of states and the dashed curves those for the minority spin. The Mo atomic concentrations are (i) 2%, (ii) 4%, (iii) 10% and (iv) 14%. The exchange splitting of the Ni d states decreases with increasing Mo concentration. The effects of exchange on Mo are very small and there is a very small induced moment on Mo atoms at low concentrations. Since we are interested in the shape of the densities of states, the figure shows them in arbitrary units scaled between 0 and 1. The Fermi energies lie in the region just above -0.2 Ryd.

Figure 2 shows the local magnetic moment in Bohr magnetons per atom as a function of the Mo concentration. The short-dashed curve shows CPA results, while the long-dashed curve shows the results from the ASR. In the low-concentration regime, the CPA consistently gives larger magnetic moments. To compare with experiment, we convert the magnetic moment to magnetization in units of kA m^{-1}. The ASR results are shown in figure 3. The experimental data of Khan *et al* [4] are shown as squares. We first note that the ASR results for the regime of very low Mo concentration agree rather well with experiment, while the CPA results are consistently higher. Khan *et al* suggest that the magnetization vanishes at around a concentration of 8% of Mo. The rigid-band model predicts a transition at around 10%, while both the CPA and the ASR predict a transition at around 12 to 13% of Mo. How do we reconcile these discrepancies? The rigid-band model

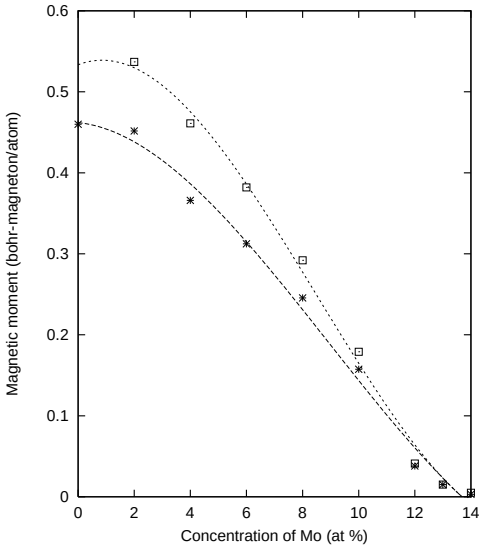

Figure 2. The magnetic moment on Ni as a function of the Mo concentration. Stars correspond to the augmented-space calculations while the squares correspond to the CPA.

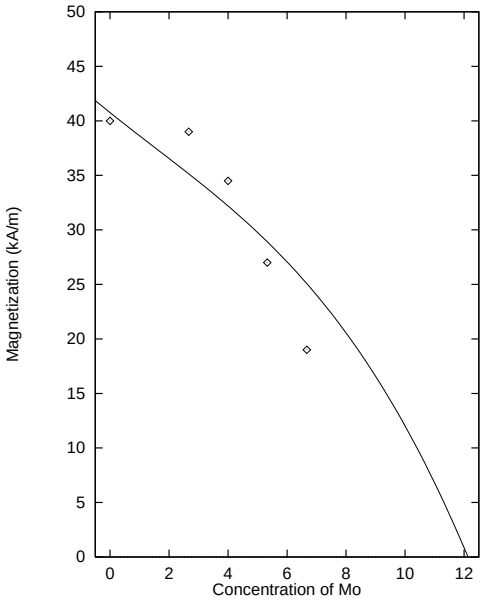

Figure 3. The magnetization as a function of the Mo concentration at 0 K obtained from the theoretical estimates.

assumes that the bands of Ni and Mo are identical but rigidly displaced from each other. Both the CPA and our ASR provide more qualitatively accurate pictures. Our theoretical results actually calculate the magnetization per atom in a ferromagnetic arrangement. Here the local and global magnetizations are the same. The experimental results yield the average global magnetization

$$m = (1/N)\sum m_{\mathrm{loc}}.$$

NiMo, like all typical spin-glass alloys, is a solid solution of a magnetic constituent, Ni, and a non-magnetic one, Mo. Therefore, as for all spin-glass alloys, we expect a paramagnetic–spin-glass transition in the concentration region 8%–13% of Mo. The experimental global magnetization experiments will show a vanishing magnetization, whereas our calculations will not show this. More detailed experiments, such as Mössbauer, low-field dc-susceptibility and hysteresis studies, need to be done for this concentration region to get a better picture. This regime promises richness and variety in magnetic behaviour.

Figure 4 plots the Curie temperature versus the concentration of Mo. Qualitatively, the behaviour is in agreement with the results of Khan *et al*. The Bragg–Williams approximation used here is known to consistently overestimate the transition temperature. These results also indicate the absence of a transition from a paramagnetic to an ordered phase at around 12% of Mo. Again, this is not surprising in the context of the discussion above. Our theoretical model also does not incorporate the possibility of a spin-disordered phase which becomes energetically favourable at around 8% Mo concentration.

We conclude by making the remark that the concentration regime 8%–14% Mo requires both more careful experimental studies as well as more elaborate theoretical models which incorporate the possibility of the spin-disordered phase as well.

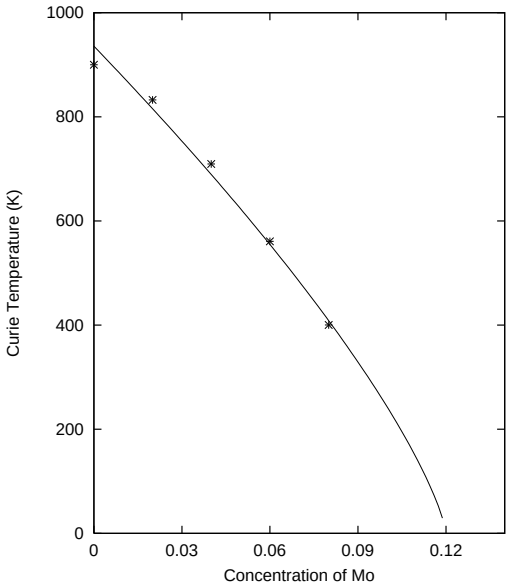

Figure 4. The Curie temperature as a function of the Mo concentration.

Acknowledgments

ND would like to thank the CSIR, India, for financial assistance. AM acknowledges useful discussions with Dr G P Das and Professor A K Majumdar.

References

[1] Das G P, Salunke H and Banerjee S 1997 *Bull. Mater. Sci.* **20** 787
[2] Andersen O K and Jepsen O 1984 *Phys. Rev. Lett.* **53** 2571
[3] Saha T, Dasgupta I and Mookerjee A 1994 *J. Phys.: Condens. Matter* **6** L245
[4] Khan F A, Asgar M A and Nordblad P 1997 *J. Magn. Magn. Mater.* **174** 121
[5] Andersen O K, Jepsen O and Krier H 1991 *Electronic Structure of Metals and Alloys* ed O K Andersen, V Kumar and A Mookerjee (Singapore: World Scientific)
[6] Dasgupta I, Saha T and Mookerjee A 1996 *J. Phys.: Condens. Matter* **8** 1979
[7] Mookerjee A and Prasad R 1985 *Phys. Rev.* B **48**
Dasgupta I, Saha T and Mookerjee A 1993 *Phys. Rev.* B **51** 17 724
[8] Saha T, Dasgupta I and Mookerjee A 1995 *J. Phys.: Condens. Matter* **7** 3413
[9] Luchini M U and Nex C M M 1987 *J. Phys. C: Solid State Phys.* **20** 3125
[10] Ghosh S, Das N and Mookerjee A 1997 *J. Phys.: Condens. Matter* **9** 10 701
[11] Ling M F, Staunton J B, Johnson D D and Pinski F J 1995 *Phys. Rev.* B **52** 3816
[12] Drchal V, Kudrnovský J and Weinberger P 1994 *Phys. Rev.* B **50** 7903
[13] Dasgupta I, Saha-Dasgupta T, Mookerjee A and Das G P 1997 *J. Phys.: Condens. Matter* **9** 3529
[14] Korzhavyi P A, Ruban A V, Abrikosov I A and Skriver H L 1995 *Phys. Rev.* B **51** 5773
[15] Ghosh S, Das N and Mookerjee A 1998 *Int. J. Mod. Phys.* B submitted
[16] Mookerjee A 1998 *Electron Correlations in Atoms and Solids* ed A N Tripathi and I Singh (New Delhi: Phoenix) pp 180–98
[17] Burke N E 1976 *Surf. Sci.* **58** 349